AGRICULTURE

Mitigation efforts will not fully alleviate the increase in water scarcity occurrence probability in wheat-producing areas

Miroslav Trnka[1,2]*, Song Feng[3]*, Mikhail A. Semenov[4], Jørgen E. Olesen[1,5,6], Kurt Christian Kersebaum[1,7], Reimund P. Rötter[8,9], Daniela Semerádová[1], Karel Klem[1], Wei Huang[10], Margarita Ruiz-Ramos[11], Petr Hlavinka[1,2], Jan Meitner[1], Jan Balek[1], Petr Havlík[12], Ulf Büntgen[1,13,14,15]

Global warming is expected to increase the frequency and intensity of severe water scarcity (SWS) events, which negatively affect rain-fed crops such as wheat, a key source of calories and protein for humans. Here, we develop a method to simultaneously quantify SWS over the world's entire wheat-growing area and calculate the probabilities of multiple/sequential SWS events for baseline and future climates. Our projections show that, without climate change mitigation (representative concentration pathway 8.5), up to 60% of the current wheat-growing area will face simultaneous SWS events by the end of this century, compared to 15% today. Climate change stabilization in line with the Paris Agreement would substantially reduce the negative effects, but they would still double between 2041 and 2070 compared to current conditions. Future assessments of production shocks in food security should explicitly include the risk of severe, prolonged, and near-simultaneous droughts across key world wheat-producing areas.

INTRODUCTION

The Food and Agriculture Organization (FAO) (*1*) has projected a 43% increase in the global annual demand for cereals from approximately 2.1 Gt in 2006 to 3.0 Gt by 2050, which is fairly conservative compared to other projections of the cereal demand (*2*). The increase in the consumption of cereals (including maize, rice, sorghum, and millet, in addition to wheat itself) will predominantly come from developing countries. Moreover, if sustainable intensification is unsuccessful in developing countries, these regions will increasingly depend on expanding net cereal imports (*3*). These developments may increase food insecurity and, consequently, political instability and migration (*4*).

Here, we focus on wheat, the world's primary rain-fed crop in terms of harvested area that is directly influenced by water scarcity (*5*). Wheat provides approximately 20% of all calories consumed by humans (*6*), the global wheat trade equals those of maize and rice combined (*6*), and drought effects have been implicated as one of the key drivers in the 2007/2008 price spike (*7*). Ten key wheat-producing regions (Fig. 1A) account for 54% of the global wheat-growing area, 57% of the global wheat production (WhP), and more than 92% of global wheat exports (*8*). Previous studies have demonstrated that global WhP strongly depends on water availability during and before the crop-specific and typically unirrigated growing season (*9*). Between 1985 and 2007, drought effects on the global WhP doubled compared to those in 1964–1984 (*9*, *10*).

Both state-of-the-art process-based (*11*) and statistical (*12*) modeling currently predict a 4.0 to 6.5% decrease in global WhP per 1°C of warming if no adaptation occurs. However, a suitable crop replacement for wheat in a drier future seems unlikely, because wheat exhibits a very low total water requirement overall (*13*) and, furthermore, is characterized by its ability to withstand substantial reductions in water availability over relatively long periods of time (*14*). These characteristics make wheat likely to remain an important crop in rain-fed crop production systems. We therefore aim to estimate the changes in the likelihood of key wheat-producing areas being simultaneously affected by major drought events as a consequence of projected future increases in drought events under different representative concentration pathways (RCPs) (*15*). To achieve this, we calculate the distribution of the global WhP area within actual agricultural land (fig. S1), account for a regional phenological calendar, and particularly model the spatial extent affected by severe water scarcity (SWS) events each year. This new water scarcity indicator combines three different time scales of the standardized precipitation evapotranspiration index (SPEI). The analysis of SWS facilitates the depiction of drought episodes that affect the entire wheat growing season, peak during its critical portion, and happen against the backdrop of long-term drought, which deplete regional water resources in general (table S1). Furthermore, we define extreme water scarcity (EWS) events to evaluate changes in the area affected by extreme levels of water scarcity that are highly unlikely under the current climate (tables S1 and S2). Our study complements

[1]Global Change Research Institute CAS, Bělidla 986/4b, Brno 603 00, Czech Republic. [2]Mendel University in Brno, Institute of Agrosystems and Bioclimatology, Zemědělská 1, Brno 613 00, Czech Republic. [3]Department of Geosciences, University of Arkansas, Fayetteville, AR, USA. [4]Plant Sciences Department, Rothamsted Research, Harpenden, Hertfordshire AL5 2JQ, UK. [5]Department of Agroecology, Aarhus University, Blichers Allé 20, 8830 Tjele, Denmark. [6]iCLIMATE Interdisciplinary Centre for Climate Change, Aarhus University, Frederiksborgvej 399, 4000 Roskilde, Denmark. [7]Leibniz-Centre for Agricultural Landscape Research, Eberswalder Str. 84, 15374 Müncheberg, Germany. [8]Tropical Plant Production and Agricultural Systems Modelling (TROPAGS), University of Göttingen, Grisebachstraße 6, 37077 Göttingen, Germany. [9]Centre of Biodiversity and Sustainable Land Use (CBL), University of Göttingen, Büsgenweg 1, 37077 Göttingen, Germany. [10]Key Laboratory of Western China's Environmental Systems (Ministry of Education), College of Earth and Environmental Sciences, Lanzhou University, Lanzhou 730000, China. [11]CEIGRAM-Universidad Politécnica de Madrid, ETSIAAB, 28040 Madrid, Spain. [12]International Institute for Applied Systems Analysis (IIASA), Schlossplatz 1, A-2361 Laxenburg, Austria. [13]Department of Geography, University of Cambridge, Downing Place CB2 3EN, UK. [14]Swiss Federal Research Institute WSL, Zürcherstrasse 111, 8903 Birmensdorf, Switzerland. [15]Department of Geography, Faculty of Science, Masaryk University, Kotlářská 2, 613 00 Brno, Czech Republic.
*Corresponding author. Email: mirek_trnka@yahoo.com (M.T.); songfeng@uark.edu (S.F.)

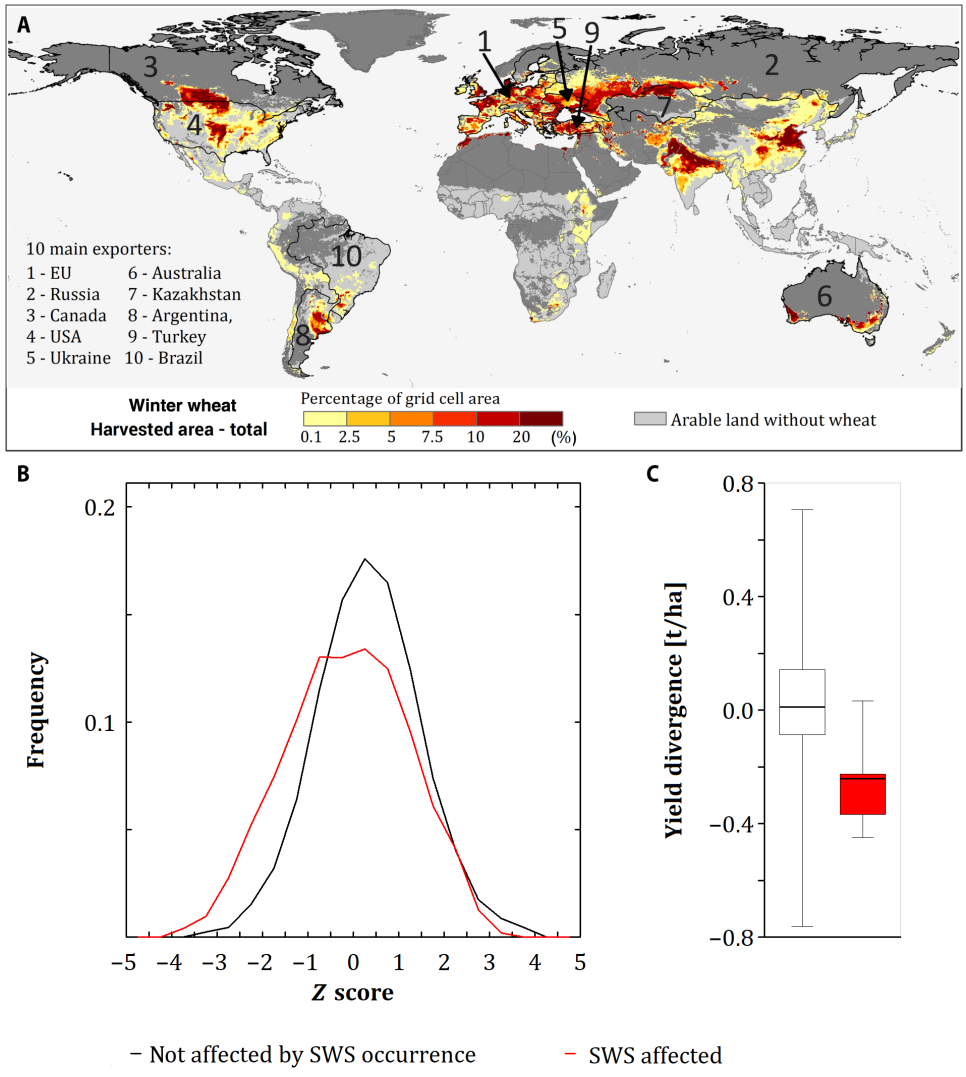

Fig. 1. Most important wheat-growing areas and the effect of SWS on wheat yields. (**A**) Colors mark the spatial distributions of the wheat-growing area and the top 10 wheat exporters during 2009–2012 in descending order, with light gray showing arable land without wheat cultivation. (**B** and **C**) Comparison of wheat yield deviations during years with and without severe water scarcity (SWS) occurrence, combining the 10 main wheat exporters [European Union (EU), Russia, Canada, United States, Ukraine, Australia, Kazakhstan, Argentina, Turkey, and Brazil]. SWS and yield data over the period 1991–2016 were used. (B) Frequency of yield deviation expressed as the *Z* score and smoothed by Gaussian filter for years with no SWS occurrence (n = 136) versus years when at least 1% of the exporter's wheat-growing area was affected by SWS (n = 78) during the year of harvest. (C) Yield differences at the exporter entity level relative to the previous year for years with no SWS occurrence (n = 136) versus years when at least 10% of the exporter's wheat-growing area was affected by SWS (n = 5).

existing crop model–based analyses that thus far have not allowed the investigation of potential synchrony in water scarcity events across the global wheat-growing area.

We use spatially and temporally coherent analyses of the global SWS risk for all wheat-growing areas, including those in developing countries and low-income regions (*16*), such as in Eastern and Southern Asia, which is where about half of today's undernourished live and where wheat accounts for a large proportion of food consumption (*17*). Recent evidence suggests that variations in crop product prices are linked to simultaneously challenging economic factors, such as oil prices and exchange rates (*18*), as well as the occurrence of large-scale droughts (*19*) and corresponding market and policy responses (*7*). This study introduces and applies a method that allows the estimation of the probability of simultaneous droughts affecting geographically distant wheat-growing areas on different spatiotemporal scales and accounting for a representative range of global climate models and emission scenarios. The results indicate a severely heightened risk of high-impact extreme events under the future climate, which would likely affect all market players, ranging from direct influences on subsistence farmers to price-mediated changes in international markets.

RESULTS

SWS versus WhP and wheat prices

We tested the hypothesis that years with an unusual SWS extent should be reflected in the WhP and be considered in wheat prices. Although such a notable relationship would not imply that SWS could or should be used to estimate wheat price anomalies, it is important to

test the SWS concept's relevance under the present climate. We use the highest spatial resolution data available to examine whether SWS occurrence has any observable relationship with WhP (Fig. 1, B and C) and price levels (figs. S2 to S4) during the baseline period. Because there were only a few events when more than 10% of the wheat-growing area of any major wheat-producing region or country was affected by SWS, we also investigated events with at least 1% SWS occurrence. This is due to the low SWS probability during the baseline. Nevertheless, we found significantly ($P < 0.01$) lower yields during SWS events than during years without SWS events (on average, 22% lower) and a markedly increased probability of very low yields during these events (Fig. 1B). These tests indicate that SWS has the capacity to account for drought-induced decreases of the wheat yield on the scale used for analyses in this paper.

In the next step, we compared the area annually affected by SWS (i) calculated over all arable land (fig. S2), (ii) weighted by the affected wheat-growing area (fig. S3), and (iii) weighted by the affected wheat-growing area of the top 10 exporters (fig. S4) with the global time-detrended (and nondetrended) wheat prices. In all cases, there was a statistically significant relationship ($P < 0.01$) between the area affected by SWS and fluctuations in the global wheat price (figs. S2 to S4). The correlation between SWS and the international wheat price is highest when the SWS area is evaluated for only the top 10 exporting countries and is the lowest when the SWS-affected area takes into account all arable land. This result again seems to favor the SWS concept, as it is reasonable to expect that markets are most sensitive to SWS events in the countries responsible for wheat exports compared to the overall wheat-growing area or even global arable land. When SWS was calculated considering the wheat-growing area of the top 10 exporters, the spatial extent of SWS explained 81% of the price fluctuations of wheat (and 24% of their first-order differences) between 2000 and 2016 (fig. S4). The explained variability decreased to 67% (and 23% in the case of the first-order differences) when the SWS extent over the global wheat-growing area was considered and to only 37% (12%) when SWS was integrated over all arable land. We are aware that dimensional approaches tend to overestimate the explanatory power of any single driver (*20*). The proportion of explained variability was smaller, i.e., 57% (22%) when a more extended period, namely the period 1990–2016, was considered. This could be related to the higher stock-to-use ratio during the period 1990–1999 than that during the period 2000–2016 (*18*), as well as to the substantial financialization of agricultural markets during the second period, both of which led to a higher sensitivity of prices to production-side shocks (*21*). The global wheat price shows similar temporal dynamics to the area affected by SWS between 1994 and 2016, including the 2007–2008 price hike (*22*), the 2010 drought in Russia, the 2012 drought in the Midwestern United States (*23*), and the subsequent period of price decreases in 2015 and 2016 (fig. S4). The relationship between SWS and international wheat prices remains statistically significant ($P < 0.001$), even when any given 1 or 2 years are discarded. This finding indicates that the results would hold even if the years of peak prices in 2007/2008 and 2010/2011 were ignored. The correlation between the extent of the wheat area (WhA) affected by SWS and international wheat prices observed over the past 20 years does not allow us to make any quantitative conclusions about the role of drought in the observed price spikes because numerous other factors were at play, such as the biofuel demand, market speculation, the stock-to-use ratio, oil prices (*18*, *20*), and policy responses or trade shocks (*7*). However, our results are in line with those of other studies [e.g., (*19*)] and confirm that production-side shocks are one of the key drivers of price variability. The results show that variations in the proposed SWS indicator are, at least to some extent, related to wheat markets, and therefore, projected shifts of the future SWS probability should be factored in when estimating future WhP variability and price levels.

Present and expected SWS extent

On average, we found that 4.5 ± 3.6% of the global wheat-growing area was affected by SWS each year between 1911 and 2016, with the maximum extent being nearly 15% in 2010 and 2012. The increase in the average area affected by SWS between 1911 and 2000 was small (0.4 percentage points per decade) yet significant ($P = 0.035$); however, this rate increased to 2.9 percentage points per decade between 2001 and 2016, coinciding with a global increase in wheat prices.

Using a landmass dataset of gridded meteorological observations (*24*) and the ensemble output from 27 global circulation models (GCMs) (table S3) (*25*), we show that, by the mid-21st century, SWS is most likely to occur in an almost continuous belt from the Iberian Peninsula in the west to Anatolia and Pakistan in the east (Fig. 2). Significant increases in SWS will also very likely affect southeastern Ukraine, southern regions of Russia, and western parts of the United States and Mexico, as well as southwestern Australia and South Africa. Meanwhile, Europe, Asia, and North America will experience a sharp upward trend in SWS (Fig. 2 and fig. S5), but South America's wheat-growing areas will be affected only marginally. Increasing SWS for the top 3 exporters, i.e., the European Union (EU), Russia, and the United States, will be significantly higher than that for the two current leading wheat importers, i.e., India and China (fig. S5, B to D). Together, the EU and Europe as a whole exhibit the largest amplitude in SWS occurrence among the different RCPs (fig. S5), indicating that WhP in these regions would benefit more than any other region from reductions in greenhouse gas (GHG) emissions. Within the EU, the highest SWS increase will occur in the drought-prone southwestern and southeastern regions of the Mediterranean (Fig. 2 and movies S1 to S3).

Although the area affected by SWS was estimated to be slightly smaller when using meteorological observations than when using GCM-based simulations of historical weather conditions, the overall differences were nonsignificant (Fig. 3A) and were mostly within the GCM model range (Fig. 3B). The observed and projected increase in the wheat-growing area affected by SWS is summarized in Fig. 3. The wheat-growing area affected by SWS over a 3-year period will increase significantly, from a mean value of 11.8 ± 4.4% during 1961–1990 to 26.8 ± 10.6% and 28.5 ± 11.7% by 2011–2040 under RCP 2.6 and RCP 8.5, respectively. This result is concerning, given the recent wheat price fluctuations in response to a much smaller area being affected by SWS. There were no significant ($\alpha = 0.01$) differences among the RCPs during 2011–2040, but the divergence among RCPs rises sharply during 2041–2070 (Fig. 3 and figs. S4 and S5). During the same period, the likelihood of widespread drought significantly increases (Fig. 3B, figs. S6 and S7, and movies S1 to S3).

According to the RCP 2.6 pathway, a reduction in emissions would considerably decrease future SWS levels in the key wheat-producing areas in the late 21st century (Fig. 3, A and B) compared to the other two RCPs, but the levels would still double. Under RCP 8.5, and even under RCP 4.5, the extent of the area affected by SWS each year is likely to rise above any observation over the past 100 years (fig. S6). If the mean area affected by SWS is considered during a 3-year window,

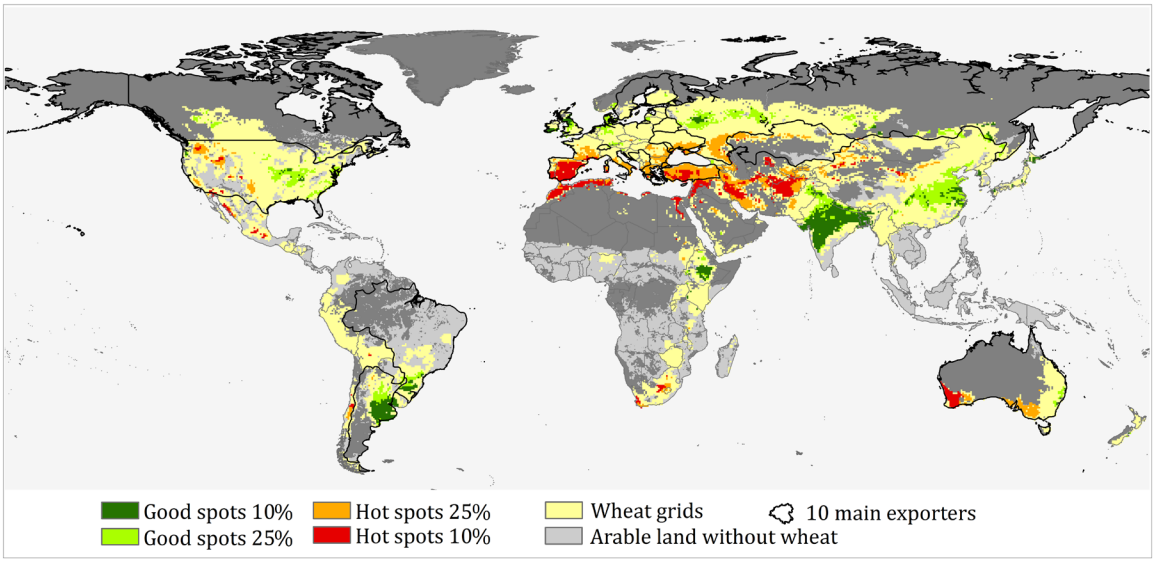

Fig. 2. Areas that are most and least at risk of an increased probability of SWS during the wheat season. The hot spots depict the 10% (or 25%) of grids with the highest SWS occurrence, which are also important wheat-producing areas. The good spots represent the 10% or 25% of wheat-producing grids with the lowest probability of SWS. The estimates are based on the analysis of the entire set of projections of 27 GCMs (table S2) for RCP 2.6, RCP 4.5, and RCP 8.5 for the period 2041–2070, which was compared with the SWS occurrence from 1961 to 1990, based on the control run using the same set of GCMs. The grids where wheat is being grown outside hot/good spots are depicted by light yellow, and light gray depicts the remaining agricultural land.

then 44.5 ± 12.3% (RCP 4.5) and 62.3 ± 13.7% (RCP 8.5) of the wheat-growing area are projected to suffer from SWS (figs. S8 and S9). Even under RCP 2.6, the median area of SWS by the end of this century surpasses all existing records since 1901.

When we consider projections for RCP 8.5 at the end of the current century, there is a significant increase in the likelihood of a sequence of 3 years during which SWS will occur across multiple key wheat-producing regions (Fig. 3B and fig. S6). The increase in the area affected by SWS in the top 10 wheat-exporting countries is significantly higher ($\alpha = 0.01$) (fig. S7), and the absolute difference in SWS levels among RCPs is particularly high when only changes in these top 10 exporting regions are considered.

DISCUSSION

The relationship between the peaks in international commodity prices observed in 2007/2008 and those observed in 2010/2011 and SWS is complex, as these spikes are a result of a "perfect storm" in the form of mutually reinforcing simultaneous developments in multiple drivers, rather than of a single isolated event [e.g., (7)]. Tadasse *et al.* (*18*) distinguished between fundamental drivers (which refer to shocks on the demand and supply side) and macro drivers (which act outside of the agricultural sector). Over time, fundamental drivers can potentially lead to reductions in the stock-to-use ratio. Macro drivers have an indirect impact on prices, for example, through costs due to exchange rate effects or energy prices. Last, the financialization of commodity markets, which refers to the unprecedented flow of capital into commodity markets, has made them subject to speculation. Within this context, our results provide unique insight into shocks on the supply side, as they coherently quantify water scarcity in terms of time and space on the global scale, including future developments of the SWS intensity, extent, and frequency across all key wheat-growing areas. Our results suggest that, even under the ambitious mitigation scenario aimed to stabilize global warming at 2°C compared to pre-industrial levels (*26*), the increase in the frequency and extent of adverse weather extremes and related shocks on the production side would be unprecedented. How much this will affect food prices and food security will depend on the development of other influencing factors.

Reaching ambitious mitigation targets will likely lead to higher energy prices and a greater demand for bioenergy—at least in the medium term (*27*). These two factors would further reinforce the impacts of SWS on wheat prices, such as the recently observed price peaks. Decoupling future production-side shocks from price spikes will thus require coordinated efforts in stock management to maintain the stock-to-use ratio at safe levels and the control of financial markets to minimize the price reaction beyond the fundamental drivers. Last, liberalized trade has often been advocated as a potentially efficient adaptation measure (*28*, *29*), while unilateral restrictive trade policies contribute to aggravating recent price spikes. A solid framework for the global coordination of trade policies will thus be necessary to allow trade to alleviate rather than exacerbate the effects of regional extremes on global markets.

Key study assumptions

It is well known that warmer temperatures will accelerate crop development, leading to earlier maturity, which creates a higher water demand per day, but the total demand depends on the length of the growing season. Therefore, projecting seasonal SWS should consider the changes in crop duration under climate change. This analysis is based on the assumption that this change will be limited to 1 month, as found in other studies (*30*). Therefore, we provide a sensitivity analysis of shifting the sowing/harvest date by 1 month (fig. S10) to ensure that the effects of changes in the crop duration and the associated water demand resulting from climate change are captured by the calculated SWS. A notable and significant drought risk reduction ($P < 0.01$ for all RCPs tested) was found in areas affected by SWS

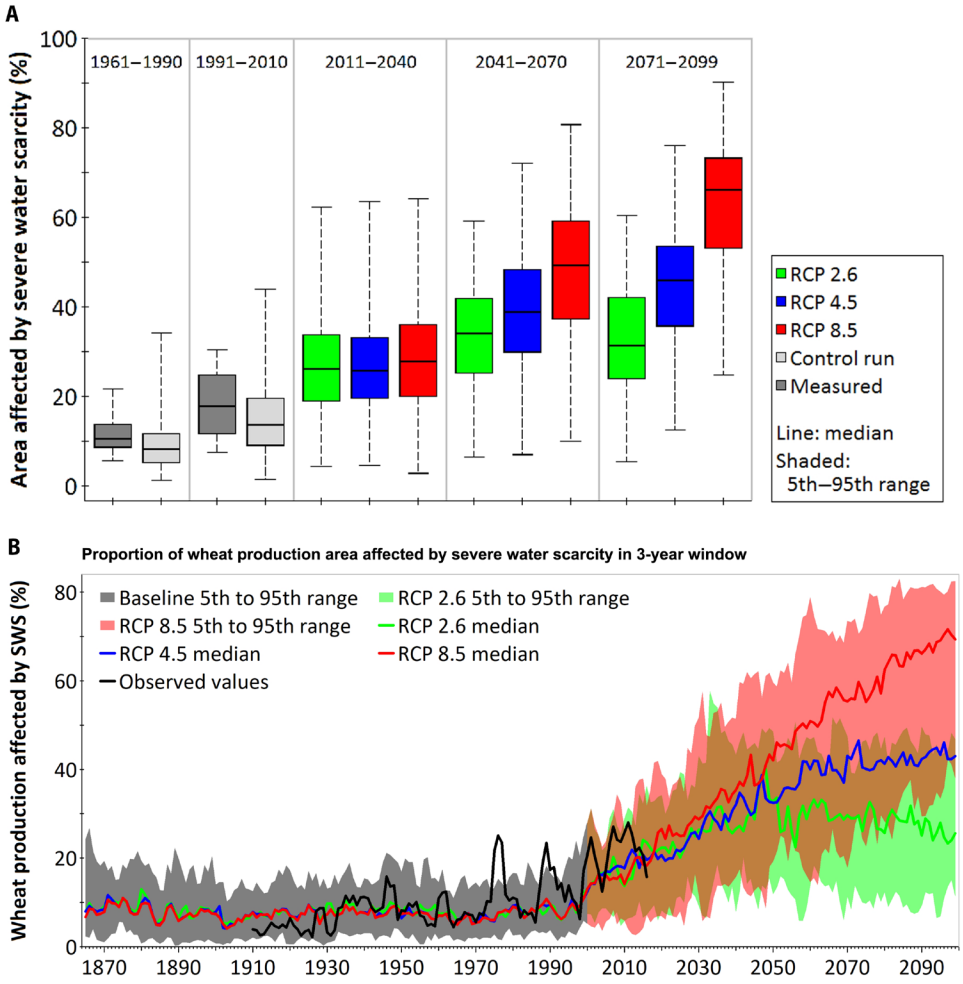

Fig. 3. Estimated proportion of global wheat-growing area affected by SWS between 1861 and 2100. (**A**) Box plots of the proportions of the global WhA affected by SWS during the harvest year or in one of the two preceding seasons, based on observed data (*12*) and GCM data (table S2) for two controls and three future time slices. (**B**) Annual values of areas affected by SWS during the harvest year or two preceding seasons using CRU-based observed data (1911–2016) and control run data (i.e., 1860–2010) (*24*) and GCM data for three RCP scenarios during the period 2011–2100.

when the harvest date was advanced by 1 month, changing from 6.0 ± 2.0% to 5.0 ± 1.8% per 1°C of warming (fig. S10). However, the advancement of the harvest date was insufficient in terms of reducing the areas of SWS to the levels experienced during 1961–1990, and such a change is also likely to decrease the yield potential, unless cultivars are adapted (*31*). Postponing the harvest by 1 month will lead to a significant ($P < 0.001$) increase in the area affected by SWS, changing from 6.0 ± 2.0% to 6.6 ± 2.2% per 1°C of warming. These changes would affect not only wheat but also entire crop rotations (*32*).

We assumed that the current wheat-growing areas and their relative weights will remain static during the entire 21st century. Therefore, we tested the potential benefit of shifting WhP to other agricultural land that has a lower SWS probability than that in current wheat-growing areas. Although the incidence of SWS over the current global arable land/agricultural land increased by 7.7%/9.8% per 1°C of global warming, the rate was fairly similar (8.5%/9.3%) over the entire or main wheat-growing areas (figs. S8 and S9). Thus, there is relatively little to be gained globally in terms of decreasing SWS exposure by shifting wheat-producing areas both within and outside the present wheat-growing area. Although we did not consider expanding the wheat-growing area to regions that are not cultivated at present because it would lead inter alia to increased CO_2 emissions (*33*), we acknowledge that these options exist.

Studies have argued that some or all the negative global warming impacts on wheat yields might be compensated for by the increasing atmospheric CO_2 concentration in combination with adaptation strategies (*32*, *34*). In semiarid environments, wheat growth will be enhanced by the higher water use efficiency under elevated CO_2 (*35*). However, the authors of the corresponding study stated that "supplemental irrigation was applied to the entire experiment on occasion during excessively dry periods to prevent crop loss," indicating that the CO_2 transpiration effect has limitations under extreme drought, as has been confirmed experimentally by Medina *et al.* (*36*). Although water use is reduced under elevated CO_2 (*37*) and may alleviate moderate dry spells, recent studies have found that drought stress mediated by severe heat cannot be compensated for by elevated CO_2 (*38*, *39*). Long-term studies with elevated CO_2 revealed that intensifying drought for some crops resulted in diminished yield stimulation under an elevated CO_2 concentration (*40*). In addition, Dai *et al.* (*41*) compared the future drying in a model simulation with and without considering

the plant physiology in response to increasing CO_2. They found that the plant physiological response to increasing GHGs is secondary, suggesting that the impact of CO_2 fertilization on future drought is small. As explained in Materials and Methods, we calculated the potential evapotranspiration (PET) through the Penman-Monteith method using an approach based on the surface energy budget, and therefore, the ambient CO_2 effects on plant transpiration, vegetation growth, and feed feedback are implicitly considered. Therefore, we postulate that the effects of SWS will likely not be alleviated by enhanced CO_2 and that SWS implementing PET based on the surface energy budget approach represents a reliable indicator of drought irrespective of CO_2 levels.

Adaptation strategies

Even the strongest mitigation efforts assumed in the RCPs will not prevent increasing SWS, and therefore, timely adaptation action is required. Strategies to reduce the impacts of water shortages on WhP could include (i) shifting the wheat growing season; (ii) full or partial irrigation; (iii) increasing the water use efficiency by, among other things, enhancing rainfall infiltration and reducing soil evaporation; and (iv) using wheat varieties with enhanced drought and heat tolerance.

Shifting the sowing and harvest dates has already been documented for adaptation [e.g., (*42*)] and is likely to be combined with the use of more resilient cultivars and management optimized for the specific environment. Another strategy for coping with water stress has been and will likely continue to be drought avoidance, e.g., shifting the harvest date to earlier (or later) in the season by shifting the sowing date and/or by using early-ripening cultivars to alleviate drought stress. Shifting the harvest time may reduce the yield losses caused by water scarcity in some regions (*43*). However, in some regions with the highest risks of increasing water scarcity within the wheat season (Fig. 2), such as the Mediterranean, this strategy has a limited scope if the dry period extends into late autumn. In addition, for temperate climates, particularly those at higher latitudes, this avoidance strategy can lead to less global radiation being intercepted by the crop [effective global radiation (EfGr)] (*44*) and, thus, a lower yield potential. Therefore, although adjusting the harvest date may be a beneficial strategy in several regions, it will most likely reduce production levels, unless the sowing date can be adjusted to maintain the EfGr.

Using drought- and heat-adapted wheat varieties seems to be a promising option; however, the breeding of enhanced drought- or heat-tolerant wheat cultivars depends on which physiological factors cause yield penalties under drought and to what extent these factors are under genetic control. Phenomic and genomic approaches need to be integrated with crop physiological investigations and ecophysiological and genetic modeling to design wheat traits for future climate conditions (*45*). These approaches should aim to exploit not only genetic variation (providing productivity gains) but also quality traits (*45*).

Irrigation represents a seemingly attractive option as well; however, dwindling water resources in some regions (*23*, *46*) cast doubt on the feasibility of irrigation being able to increase wheat yield on a global scale without massive investment programs. Therefore, developing management strategies to improve field conditions in a bid to increase drought resilience is crucial. For example, in the Mediterranean, the application of only one supplementary irrigation event during sensitive stages in combination with the selection of an optimized sowing date and cycle duration can maximize the grain filling length while preventing environmental stressors at both the end (at sowing) and the beginning (at grain filling) of the dry summer period (*47*). Deficit irrigation is a common on-farm water-saving strategy, which involves irrigating crops below the requirements defined by evapotranspiration (*48*). In general, this approach aims to increase the water use efficiency while minimizing reductions in crop yields and saving available water resources. Although deficit irrigation can improve the water use efficiency and may reduce the total withdrawals for irrigation, the consumptive use of water may also increase, thereby reducing return flows and causing negative groundwater balances [see, e.g., (*49*)], which may increase the risk of salinization in arid regions.

Another option that should be considered is soil management focused on building up the soil water for the next crop. This is partially possible by conserving water through minimizing tillage and reducing nonproductive water loss (i.e., evaporation) (*50*) from the unshaded soil surface. The latter can be achieved by covering the soil surface with a mulch of plant residues or plastic, which reduces evaporative water losses (*51*). Water use can be further improved by water harvesting approaches, where water is captured in the soil or by water reservoirs located on the farm or in the catchment for later use by crops (*52*). There are many approaches that can be implemented to enhance water harvesting and management, and these methods need to be tailored to the local landscape, soil, and climatic conditions. In addition, possible adaptations usually have other implications (e.g., forcing changes in crop rotation) and thus should not be considered as cost-free strategies, as rightly noted by Lobell (*32*).

The suitability of a given adaptation measure will vary on the basis of the climate and soil conditions, as well as the type and timing of the drought event. If the variability in drought timing increases (in addition to the frequency and severity, as shown above), then it will further complicate decision-making and the efficient use of adaptation measures. Integrated strategies for entire catchments have rarely been introduced so far because of governance complexities, although this is potentially the most efficient approach.

Our understanding of the impacts of climate change on agricultural prices has relied to a large degree on global agricultural market models. These models also include the potential of incremental adaptations that rely on currently available management systems and crop varieties. Leclère *et al.* (*28*) found in a single-model study that, without adaptation, the total crop calorie loss would reach up to 18% by 2050. Incremental adaptation achieved by selecting an appropriate management system, relocating crop production to more suitable or less negatively affected areas, and expanding the crop area could buffer 17, 44, and 22% of the negative climate effect, resulting in a residual calorie availability decrease due to climate change of only 3%. Similar results were found in a multimodel study by Nelson *et al.* (*53*), who also considered the impacts on agricultural prices and highlighted the idea that adaptation would lead to an average of 20% increase in crop prices. However, these studies considered only gradual changes in yields due to climate change, and to the best of our knowledge, no studies have assessed the economic potential for adaptation to an increased frequency of extreme weather events.

Although even major mitigation efforts (represented by RCP 2.6) do not prevent the doubled risk of SWS simultaneously affecting wheat-growing areas, it certainly makes the increase more manageable, especially in comparison with the increases projected under RCP 8.5. Limiting global warming by the end of 2100 to +1.5°C instead of the targeted 2.0°C threshold would reduce the mean area affected by SWS by approximately 3% (figs. S8 and S9), which significantly exceeds the potential achieved by all possible shifts in the wheat growing season (fig. S10). Reported changes in SWS levels and the

apparent sensitivity of wheat prices to SWS increases should be considered, together with reports on dwindling water resources across many wheat-growing regions (*46*, *54*, *55*).

To meet the projected increase in the global food demand, a sustained annual yield increase of 2.4% (*56*), in contrast to the current rate of 0.9%, will be needed. Although there are estimates that a 71% increase in the potential global yield is feasible through yield gap closure (*57*), it was thought that this increase would mainly come from the expansion of irrigated areas and from enhancing nitrogen fertilization in some production regions. The increased probability of SWS years reported in this study would, in many regions, constrain efforts to increase irrigated areas but would also lead to a lower nutrient use efficiency. The efficacy and feasibility of available adaptation options should therefore be interpreted with caution and should account for changes in the SWS probability in combination with other adverse factors to avoid what has been coined "adaptation illusion" (*32*).

Our study has performed analyses to assess the probability of simultaneous large-scale severe and extreme drought across the globe during critical wheat development phases and has shown an increasing risk for global WhP as a whole. Even ambitious climate change mitigation efforts would not fully alleviate the increased risk. To fully quantify the impacts of large-scale water scarcity events on WhP and the effects of potential adaptation strategies, additional factors such as information on soil characteristics, water resources for irrigation, and the capacity of markets to absorb drought-induced production anomalies need to be included. Process-based or statistical modeling approaches can be used, although recent ensemble model studies revealed large uncertainties in the assessment of the climate change impact on crop production (*11*, *12*). Moreover, increasing competition for water use between different sectors must be considered, which has implications not only for crop production but also for regional conflicts concerning water use. The results of our study underline the urgent need for concerted global efforts to limit global warming within the targets of the Paris Agreement.

MATERIALS AND METHODS

The total area of WhP is unevenly distributed across the world, with several relatively well-defined production regions within the global arable land (fig. S1). An increase in water scarcity events in these regions might significantly increase the probability of key wheat-producing areas simultaneously (or near simultaneously) experiencing SWS or EWS (*15*). Therefore, we analyzed the likelihood of multiple wheat-producing areas experiencing SWS and EWS events during the same harvest year. In each region, we analyzed the water scarcity (as defined in table S1) occurrence over either the 4 months preceding the local harvest date or, alternatively, between the usual regional-specific sowing and harvest dates. The probability of SWS/EWS events between 1861 and 2100 was based on the SPEI (*58*). We used a global grid and defined a location within the grid as an area affected by water scarcity if both the short-term SPEI affecting WhP and the long-term SPEI affecting water resource availability occurred in a given grid cell with water scarcity conditions based on the above predefined magnitudes (table S2). The SWS/EWS probability from 1861 to 2100 was estimated using the outputs of 27 climate models from the fifth phase of the Coupled Model Intercomparison Project (CMIP5) (table S3). Occurrences of SWS/EWS during the period 1901–2016 were evaluated using the Climate Research Unit (CRU) dataset, which represent the "observed" SWS/EWS (*24*). We examined the SWS/EWS occurrences under three RCPs: (i) RCP 2.6, corresponding to the implementation of the 2015 Paris Agreement (*26*); (ii) RCP 4.5; and (iii) a high-end emission scenario, i.e., RCP 8.5. This approach allowed us to examine how climate change mitigation would affect future drought risk across the major wheat-producing regions (*59*).

Our study first considered all grids (fig. S1A) where wheat is grown (i.e., wheat grids) (*60*), with weights assigned to each grid according to the acreage of arable land and production within the respective grid. We also weighted each grid (fig. S1, B and C) on the basis of its share of the total WhA. Last, we based the grid weight on the importance of each grid in terms of the global WhP. The wheat grids constituted areas where wheat was produced in 2000 (*54*), and we assumed that these weights represented how the SWS/EWS risk would change if the wheat-growing conditions remained as they were in the year 2000. WhA and WhP weighting allowed us to examine how changes in water scarcity affected the risk in the current primary production areas based on either area or production. To analyze changes in the SWS/EWS patterns in the top exporting regions, we examined the SWS/EWS probability for grids located in the territories of the 10 most important wheat exporters, and we weighted the grids according to their share of the entire production area (WhAEx) and the production quantity (WhPEx) of wheat. Similar analyses were also conducted for the top five producers and for individual continents. The data were obtained from FAO Corporate Statistical Database (FAOSTAT) (*6*) and U.S. Department of Agriculture (*8*). These steps and data are described in detail below.

WhP area

The WhP area was determined for each 5″ grid (~10 km) on the basis of the datasets developed by Hoekstra *et al.* (*54*). For these datasets, the total acreage of arable land in each grid was first estimated and then used to estimate the share of wheat over the global WhA, and these results are presented in fig. S1. First, we selected grids where wheat has been grown, and we weighted each grid on the basis of the area of arable land within the grid. This value represented the current potential area for WhP (i.e., wheat grids), and latitudinal changes in the grid area were considered. Then, weights were assigned to each wheat grid on the basis of the proportion of the total global wheat-growing area of 210×10^6 hectares represented by a given grid. This approach allowed us to estimate how much of the global WhA was affected by SWS/EWS during each harvest year. A similar approach was applied to estimate weights according to the share of global WhP (570×10^6 metric tons) represented by each grid (i.e., WhP). The WhP of the land area mass of a grid cell was used on the basis of FAOSTAT 1999–2013 mean yield data (on the national or regional level). These data were used to derive the weights. Last, on the basis of the FAOSTAT database, the top 10 exporting regions during 2009–2012 (fig. S1) were determined, and the wheat-producing grids were weighted separately (WhAEx and WhPEx) in these countries, as shown in Fig. 1 and fig. S1. For each grid cell, the long-term mean harvest and sowing dates were estimated on the basis of data provided by Sacks *et al.* (*61*).

Climate data

We analyzed simulations from 27 global climate models (table S3) from the CMIP5 database (*25*). These simulations included model runs with specific historical, natural, and anthropogenic forcings from

1861 to 2005 and included 21st century changes in anthropogenic aerosols and GHGs following the RCP 2.6, RCP 4.5, and RCP 8.5 scenarios (*59*). If a model had multiple ensemble simulations, then we analyzed only the first ensemble run. All the monthly modeled data (e.g., temperature, precipitation, wind speed, solar radiation, and relative humidity) were first interpolated from the original model grids to a common grid with half-degree resolution and then bias-corrected using the delta method (*62*). Temperature and precipitation were bias-corrected on the basis of the observed 1961–1990 monthly climatology developed by the Climate Prediction Center (CPC) (*63*), whereas the other variables were bias-corrected on the basis of the observed 1961–1990 monthly climatology data developed by the CRU of the University of East Anglia (*64*). This bias correction method ensured that the modeled variables had the same monthly climatology as the observations from CPC or CRU during the period 1961–1990.

In addition to the model simulations, the 0.5° gridded monthly observed temperature, precipitation, and PET datasets developed by the CRU (i.e., CRU-TS.3.25) (*24*) were used. These datasets were based on observations collected from thousands of weather stations around the globe from 1901 to 2016. Therefore, the CRU datasets can be used to evaluate the CMIP5 models.

A comparison of the SWS/EWS data for the period 1861–2010 from the climate models, i.e., the "control run" data from the ensemble of the CMIP5 climate models (table S3), with the CRU-based calculations over the same time period showed very good agreement in terms of various SWS characteristics (e.g., Fig. 3 and figs. S6 and S8). The CRU-based SWS within the 95% confidence interval of the CMIP5 simulations (fig. S6) showed very similar return probabilities of SWS events (Fig. 3B). Annual visualizations of the extent of SWS based on CRU (1901–2016) data and the GCMs (1861–2100) are available as part of the Supplementary Materials. The EWS data are available from the authors.

Standardized precipitation evapotranspiration index

To evaluate changes in the occurrence of water scarcity, this study used the SPEI (*58*). The SPEI is a multiscalar drought index that quantifies drought intensity on various time scales. The SPEI can be computed on the basis of 1, 3, 6, 9, or 12 months of accumulated surface water deficits and surpluses (i.e., precipitation minus PET). The calculation then uses statistical probability distributions to quantify the drought intensity, termed the 1-, 3-, 6-, 9-, or 12-month SPEI, respectively. The 1-month SPEI is closely related to the shallow layer soil moisture and can be used to evaluate short-term drought variability. The 12-month SPEI is closely related to the deep layer soil moisture and long-term drought variability.

In this study, the PET was estimated using the physically based Penman-Monteith method [PET_PM; (*65*)], which accounts for the impacts of temperature, relative humidity, wind speed, and solar radiation. We applied an approach that derives PET_PM from the surface energy budget (i.e., Rn-G = SH + LH), where Rn, G, SH, and LH are the net radiation, ground heat flux, and sensible and latent heat flux, respectively (*66*). The CO_2 increase, vegetation growth and feedback, and CO_2 effect on plant transpiration can all influence the surface energy budget in the future. Because the PET_PM is based on the surface energy budget, the CO_2 effects on plant transpiration, vegetation growth, and feed feedback were implicitly considered by the PET_PM. In addition to consistent warming (*67*), the models were also consistent in showing regional changes in relative air humidity (*68*). The roles of wind speed and solar radiations in PET are secondary (*69*) in the future. Because of the strong impacts of temperature and relative humidity, the climate models project consistently increasing PET. This finding is understandable because the future climate is expected to be dominated by the radiative effects of increasing GHGs.

The 1-, 3-, 6-, 9-, and 12-month SPEI values were calculated on the basis of the monthly precipitation and PET. The snow-melting module developed by Van der Schrier *et al.* (*70*) was also tested to quantify the impact of snow on water supplies. However, the differences between SWS/EWS with and without considering snow melt were not significant over the wheat-growing areas. A simplified scheme that did not account for snow melting was therefore implemented. For a given climate model output, the statistical probability distribution parameters (*58*) used to calculate the SPEI were determined on the basis of the modeled monthly data from 1901 to 2000. These parameters were subsequently used to calculate the SPEI values for this grid cell from 1860 to 2005 and under different future scenarios. The same procedures were applied to calculate the SPEI from 1901 to 2016 based on the CRU dataset.

Defining severe and EWS events and drought-sensitive periods

SWS and EWS events (table S1) were first defined to quantify the short- and long-term impacts of water shortage on crops. A grid cell was considered to be affected by water scarcity only if both the short-term water scarcity indicators (i.e., 1- and 3-month SPEI) and the long-term water scarcity indicators (i.e., 12-month SPEI) reached predefined thresholds (table S1). The thresholds were adopted on the basis of Blauhut *et al.* (*71*), where the probability of drought impact occurrence was estimated on the basis of the impacts of drought on individual sectors. Because wheat is only grown during part of the year, we used two specific water scarcity sensitivity periods (SPs):

1) The wheat growing season, i.e., from the usual regionally specific month of sowing to the month of harvest. In regions where both spring and winter wheat were grown, the sowing date of the prevailing wheat season was analyzed.

2) Four months before the usual wheat harvest, i.e., the period that included both the peak vegetative stage (before the heading) and grain filling. Both stages are very sensitive to soil moisture deficits. These four months constitute the time of the most intense growth, including the formation of all yield components.

When the usual harvest date was on or later than the 20th day of the month, the drought index for the month of harvest and the three preceding months was used. When wheat was harvested before the 20th day of the harvest month, the drought index for the 4 months before the month of harvest was used. This offset was used because the harvest date of wheat, in practice, follows the physiological maturity of wheat by several days or even weeks, and the sensitivity of wheat to drought decreases rapidly at the end of the grain filling stage and postmaturity. Drier conditions during harvest are generally beneficial for wheat quality and could increase the efficiency of the harvest. In all calculations, calendar months were used.

The overall differences in drought indexes resulting from using the different SPs (fig. S7) were small and, at most, five percentage points during the control run. Therefore, a 4-month SP was primarily used in the study, as it allowed us to consider water scarcity over the same length of time across all wheat-growing regions. In most cases, the area affected by water scarcity was larger when the SP was defined from sowing to harvest, rather than as the 4 months before harvest.

Final weighting procedure

For each wheat-growing grid cell and year, we first determined whether the cell and year were affected by SWS or EWS ($D_i = 1$) or were not affected by SWS or EWS ($D_i = 0$) during each wheat growing season, on the basis of the thresholds defined in table S2. For a 1-year window of water scarcity, we considered only the events during the year of harvest. For a 2-year SWS/EWS window, the grid was considered to be affected by water scarcity ($D_i = 1$) if SWS/EWS thresholds were met either in the harvest year or during the previous harvest year. Similarly, a 3-year window of water scarcity categorized a grid as experiencing SWS/EWS if conditions were met during the SPs of the harvest year or the two preceding years. The use of the 1-, 2-, and 3-year windows allowed us to examine the impacts of a sequence of SWS (EWS) events on WhP (e.g., the 2010 droughts in Russia and India and the 2012 drought in the United States). The area affected by severe or extreme drought was then determined as follows

$$\text{Area affected by drought} = 100 * \frac{\sum_{i=1}^{n} D_i * w_i}{\sum_{i=1}^{n} w_i} \quad (1)$$

where weight w_i is the share of the global WhA (for WhA calculations) or global WhP. We also accounted for variations in grid size due to latitude.

SUPPLEMENTARY MATERIALS

Supplementary material for this article is available at http://advances.sciencemag.org/cgi/content/full/5/9/eaau2406/DC1

Table S1. Definitions of SWS and EWS for the present study.
Table S2. Return period of SWS and EWS (as defined in table S1), calculated as the average ± SD across all grids included in the global wheat-growing area (fig. S1) for the year of harvest and as the cumulative value for the harvest year and the preceding year.
Table S3. A list of the CMIP5 GCMs used in this study (with brief descriptions).
Table S4. Symbols for weighting schemes used in the paper.
Fig. S1. Weights of grids as used in the study.
Fig. S2. Relationship between the proportion of the global arable land affected by severe water scarcity (SWS) and the cereal price index.
Fig. S3. Relationship between the proportion of the global wheat growing area affected by severe water scarcity (SWS) and the cereal price index.
Fig. S4. Relationship between the proportion of the wheat growing area of the top ten wheat exporters affected by severe water scarcity (SWS) and the cereal price index.
Fig. S5. Change in the wheat production area (WhA) affected by severe/extreme water scarcity for the major world areas and the five main producers.
Fig. S6. Extent of wheat production affected by severe water scarcity for the harvest year (a) and the harvest and preceding year(s) (b) for the period from 1861 to 2100.
Fig. S7. Area affected by severe water scarcity for two different definitions of wheat sensitive period.
Fig. S8. Changes in median/maximum wheat area affected by severe and extreme water scarcity expressed as absolute change and change per 1°C global temperature increase for period 2041–2070.
Fig. S9. Changes in median/maximum wheat area affected by severe and extreme water scarcity occurring expressed as absolute change and change per 1°C global temperature increase for period 2071–2099.
Fig. S10. Comparison of area affected by severe and extreme water scarcity when future harvest is shifted by ±1 month.
Movie S1. The annual extent of SWS events for the period 1901–2016 based on the CRU data and then projections for six GCM models under the RCP 2.6 scenario.
Movie S2. The annual extent of SWS events for the period 1901–2016 based on the CRU data and then projections for six GCM models under the RCP 4.5 scenario.
Movie S3. The annual extent of SWS events for the period 1901–2016 based on the CRU data and then projections for six GCM models under the RCP 8.5 scenario.

REFERENCES AND NOTES

1. N. Alexandratos, J. Bruinsma, *World Agriculture Towards 2030/2050: The 2012 Revision* (Food Agri Org United Nations, Rome, 2012).
2. D. Tilman, C. Balzer, J. Hill, B. L. Befort, Global food demand and the sustainable intensification of agriculture. *Proc. Natl. Acad. Sci. U.S.A.* **108**, 20260–20264 (2011).
3. M. K. van Ittersum, L. G. J. van Bussel, J. Wolf, P. Grassini, J. van Wart, N. Guilpart, L. Claessens, H. de Groot, K. Wiebe, D. Mason-D'Croz, H. Yang, H. Boogaard, P. A. J. van Oortf, M. P. van Loon, K. Saito, O. Adimo, S. Adjei-Nsiah, A. Agali, A. Bala, R. Chikowo, K. Kaizzi, M. Kouressy, J. H. J. R. Makoi, K. Ouattara, K. Tesfaye, K. G. Cassman, Can sub-Saharan Africa feed itself? *Proc. Natl. Acad. Sci. U.S.A.* **113**, 14964–14969 (2016).
4. J. von Braun, *The World Food Situation: New Driving Forces and Required Actions* (Food Policy Report, Washington, DC, 2008).
5. B. Leff, N. Ramankutty, J. A. Foley, Geographic distribution of major crops across the world. *Global Biogeochem. Cy.* **18**, 1–27 (2004).
6. FAOSTAT, www.fao.org/faostat/en/#data [accessed 7 February 2017].
7. D. Headey, Rethinking the global food crisis: The role of trade shocks. *Food Policy* **36**, 136–146 (2011).
8. USDA, https://apps.fas.usda.gov/psdonline/app/index.html#/app/advQuery [acccessed 30 March 2017].
9. M. Zamperi, A. Ceglar, F. Dentener, A. Toreti, Wheat yield loss attributable to heat waves, drought and water excess at the global, national and subnational scales. *Environ. Res. Lett.* **12**, 064008 (2017).
10. C. Lesk, P. Rowhani, N. Ramankutty, Influence of extreme weather disasters on global crop production. *Nature* **529**, 84–87 (2016).
11. S. Asseng, F. Ewert, P. Martre, R. P. Rötter, D. B. Lobell, D. Cammarano, B. A. Kimball, M. J. Ottman, G. W. Wall, J. W. White, M. P. Reynolds, P. D. Alderman, P. V. V. Prasad, P. K. Aggarwal, J. Anothai, B. Basso, C. Biernath, A. J. Challinor, G. De Sanctis, J. Doltra, E. Fereres, M. Garcia-Vila, S. Gayler, G. Hoogenboom, L. A. Hunt, R. C. Izaurralde, M. Jabloun, C. D. Jones, K. C. Kersebaum, A.-K. Koehler, C. Müller, S. N. Kumar, C. Nendel, G. O'Leary, J. E. Olesen, T. Palosuo, E. Priesack, E. E. Rezaei, A. C. Ruane, M. A. Semenov, I. Shcherbak, C. Stöckle, P. Stratonovitch, T. Streck, I. Supit, F. Tao, P. J. Thorburn, K. Waha, E. Wang, D. Wallach, J. Wolf, Z. Zhao, Y. Zhu, Rising temperatures reduce global wheat production. *Nat. Clim. Change* **5**, 143–147 (2015).
12. B. Liu, S. Asseng, C. Müller, F. Ewert, J. Elliott, D. B. Lobell, P. Martre, A. C. Ruane, D. Wallach, J. W. Jones, C. Rosenzweig, P. K. Aggarwal, P. D. Alderman, J. Anothai, B. Basso, C. Biernath, D. Cammarano, A. Challinor, D. Deryng, G. De Sanctis, J. Doltra, E. Fereres, C. Folberth, M. Garcia-Vila, S. Gayler, G. Hoogenboom, L. A. Hunt, R. C. Izaurralde, M. Jabloun, C. D. Jones, K. C. Kersebaum, B. A. Kimball, A.-K. Koehler, S. N. Kumar, C. Nendel, G. J. O'Leary, J. E. Olesen, M. J. Ottman, T. Palosuo, P. V. Vara Prasad, E. Priesack, T. A. M. Pugh, M. Reynolds, E. E. Rezaei, R. P. Rötter, E. Schmid, M. A. Semenov, I. Shcherbak, E. Stehfest, C. O. Stöckle, P. Stratonovitch, T. Streck, I. Supit, F. Tao, P. Thorburn, K. Waha, G. W. Wall, E. Wang, J. W. White, J. Wolf, Z. Zhao, Y. Zhu, Similar estimates of temperature impacts on global wheat yield by three independent methods. *Nat. Clim. Change* **6**, 1130–1136 (2016).
13. R. Ortiz, K. D. Sayre, B. Govaerts, R. Gupta, G. V. Subbarao, T. Ban, D. Hodson, J. M. Dixon, J. I. Ortiz-Monasterio, M. Reynolds, Climate change: Can wheat beat the heat? *Agric. Ecosyst. Environ.* **126**, 46–58 (2008).
14. S. Daryanto, L. Wang, P.-A. Jacinthe, Global synthesis of drought effects on maize and wheat production. *PLOS ONE* **11**, e0156362 (2016).
15. A. Dai, Increasing drought under global warming in observations and models. *Nat. Clim. Change* **3**, 52–58 (2013).
16. T. Wheeler, J. von Braun, Climate change impacts on global food security. *Science* **341**, 508–513 (2013).
17. FAO, IFAD, UNICEF, WFP, WHO, *The State of Food Security and Nutrition in the World 2018. Building Climate Resilience For Food Security and Nutrition* (FAO, Rome, 2018).
18. G. Tadasse, B. Algieri, M. Kalkuhl, J. von Braun, Drivers and triggers of international food price spikes and volatility. *Food Policy* **47**, 117–128 (2014).
19. J. Schewe, C. Otto, K. Frieler, The role of storage dynamics in annual wheat prices. *Environ. Res. Lett.* **12**, 054005 (2017).
20. J. Baffes, T. Haniotis, *What Explains Agricultural Price Movements? Policy Research Working Paper, No. WPS 7589* (World Bank Group,Washington, D.C., 2016).
21. J. von Braun, G. Tadasse, *Global Food Price Volatility and Spikes: An Overview of Costs, Causes, and Solutions, ZEF- Discussion Papers on Development Policy No. 161* (Center for Development Research, Bonn, 2012).
22. G. Tadasse, B. Algieri, M. Kalkuhl, J. von Braun, Drivers and triggers of international food price spikes and volatility, in *Food Price Volatility and Its Implications for Food Security And Policy*, M. Kalkuhl, J. von Braun, M. Torero Eds. (Springer, 2016).
23. U. Chung, S. Gbegbelegbe, B. Shiferaw, R. Robertson, J. I. Yun, K. Tesfaye, G. Hoogenboom, K. Sonder, Modeling the effect of a heat wave on maize production in the USA and its implications on food security in the developing world. *Weather Clim. Extrem.* **5**, 67–77 (2014).
24. I. Harris, P. D. Jones, T. J. Osborn, D. H. Lister, Updated high-resolution grids of monthly climatic observations–The CRU TS3.10 Dataset. *Int. J. Climatol.* **34**, 623–642 (2014).
25. K. E. Taylor, R. J. Stouffer, G. A. Meehl, An overview of CMIP5 and the experiment design. *Bull. Am. Meteorol. Soc.* **93**, 485–498 (2012).

26. H. J. Schellnhuber, S. Rahmstorf, R. Winkelmann, Why the right climate target was agreed in Paris. *Nat. Clim. Change* **6**, 649–653 (2016).
27. A. Popp, K. Calvin, S. Fujimori, P. Havlik, F. Humpenöder, E. Stehfest, B. L. Bodirsky, J. P. Dietrich, J. C. Doelmann, M. Gusti, T. Hasegawa, P. Kyle, M. Obersteiner, A. Tabeau, K. Takahashi, H. Valin, S. Waldhoff, I. Weindl, M. Wise, E. Kriegler, H. Lotze-Campen, O. Fricko, K. Riahi, P. D. van Vuuren, Land-use futures in the shared socio-economic pathways. *Glob. Environ. Chang.* **42**, 331–345 (2017).
28. D. Leclère, P. Havlík, S. Fuss, E. Schmid, A. Mosnier, B. Walsh, H. Valin, M. Herrero, N. Khabarov, M. Obersteiner, Climate change induced transformations of agricultural systems: Insights from a global model. *Environ. Res. Lett.* **9**, 124018 (2014).
29. A. Mosnier, M. Obersteiner, P. Havlík, E. Schmid, N. Khabarov, M. Westphal, H. Valin, S. Frank, F. Albrecht, Global food markets, trade and the cost of climate change adaptation. *Food Secur.* **6**, 29–44 (2014).
30. A. Zimmermann, H. Webber, G. Zhao, F. Ewert, J. Kros, J. Wolf, W. Britz, W. de Vries, Climate change impacts on crop yields, land use and environment in response to crop sowing dates and thermal time requirements. *Agr. Syst.* **157**, 81–92 (2017).
31. M. Trnka, R. P. Rötter, M. Ruiz-Ramos, K. C. Kersebaum, J. E. Olesen, Z. Žalud, M. A. Semenov, Adverse weather conditions for European wheat production will become more frequent with climate change. *Nat. Clim. Change* **4**, 637–643 (2014).
32. D. B. Lobell, Climate change adaptation in crop production: Beware of illusions. *Glob. Food Sec.* **3**, 72–76 (2014).
33. P. C. West, H. K. Gibbs, C. Monfreda, J. Wagner, C. C. Barford, S. R. Carpenter, J. A. Foley, Trading carbon for food: Global comparison of carbon stocks vs. crop yields on agricultural land. *Proc. Natl. Acad. Sci. U.S.A.* **107**, 19645–19648 (2010).
34. A. J. Challinor, J. Watson, D. B. Lobell, S. M. Howden, D. R. Smith, N. Chhetri, A meta-analysis of crop yield under climate change and adaptation. *Nat. Clim. Change* **4**, 287–291 (2014).
35. G. J. Fitzgerald, M. Tausz, G. O'Leary, M. R. Mollah, S. Tausz-Posch, S. Seneweera, I. Mock, M. Löw, D. L. Partington, D. McNeil, R. M. Norton, Elevated atmospheric [CO_2] can dramatically increase wheat yields in semi-arid environments and buffer against heat waves. *Glob. Chang. Biol.* **22**, 2269–2284 (2016).
36. S. Medina, R. Vicente, A. Amador, J. L. Araus, Interactive effects of elevated [CO2] and water stress on physiological traits and gene expression during vegetative growth in four durum wheat genotypes. *Front. Plant Sci.* **7**, 1738 (2016).
37. R. Manderscheid, H.-J. Weigel, Drought stress effects on wheat are mitigated by atmospheric CO_2 enrichment. *Agron. Sustain. Dev.* **27**, 79–87 (2007).
38. Z. Jin, E. A. Ainsworth, A. D. B. Leakey, D. B. Lobell, Increasing drought and diminishing benefits of elevated carbon dioxide for soybean yields across the US Midwest. *Glob. Chang. Biol.* **24**, e522–e533 (2018).
39. B. Schauberger, S. Archontoulis, A. Arneth, J. Balkovic, P. Ciais, D. Deryng, J. Elliott, C. Folberth, N. Khabarov, C. Müller, T. A. M. Pugh, S. Rolinski, S. Schaphoff, E. Schmid, X. Wang, W. Schlenker, K. Frieler, Consistent negative response of US crops to high temperatures in observations and crop models. *Nat. Commun.* **8**, 13931 (2017).
40. S. B. Gray, O. Dermody, S. P. Klein, A. M. Locke, J. M. McGrath, R. E. Paul, D. M. Rosenthal, U. M. Ruiz-Vera, M. H. Siebers, R. Strellner, E. A. Ainsworth, C. J. Bernacchi, S. P. Long, D. R. Ort, A. D. B. Leakey, Intensifying drought eliminates the expected benefits of elevated carbon dioxide for soybean. *Nat. Plants* **2**, 16132 (2016).
41. A. Dai, T. Zhao, J. Chen, Climate change and drought: A precipitation and evaporation perspective. *Curr. Clim. Change Rep.* **4**, 301–312 (2018).
42. J. E. Olesen, M. Trnka, K. C. Kersebaum, A. O. Skjelvåg, B. Seguin, P. Peltonen-Sainio, F. Rossi, J. Kozyra, F. Micale, Impacts and adaptation of European crop production systems to climate change. *Eur. J. Agron.* **34**, 96–112 (2011).
43. M. A. Semenov, P. R. Shewry, Modelling predicts that heat stress, not drought, will increase vulnerability of wheat in Europe. *Sci. Rep.* **1**, 66 (2011).
44. M. Trnka, J. E. Olesen, K. C. Kersebaum, A. O. Skjelvåg, J. Eitzinger, B. Seguin, P. Peltonen-Sainio, R. Rötter, A. Iglesias, S. Orlandini, M. Dubrovský, P. Hlavinka, J. Balek, H. Eckersten, E. Cloppet, P. Calanca, A. Gobin, V. Vučetić, P. Nejedlik, S. Kumar, B. Lalic, A. Mestre, F. Rossi, J. Kozyra, V. Alexandrov, D. Semerádová, Z. Žalud, Agroclimatic conditions in Europe under climate change. *Glob. Change Biol.* **17**, 2298–2318 (2011).
45. R. K. Varshney, R. Tuberosa, F. Tardieu, Progress in understanding drought tolerance: From alleles to cropping systems. *J. Exp. Bot.* **69**, 3175–3179 (2018).
46. J. Elliott, D. Deryng, C. Müller, K. Frieler, M. Konzmann, D. Gerten, M. Glotter, M. Flörke, Y. Wada, N. Best, S. Eisner, B. M. Fekete, C. Folberth, I. Foster, S. N. Gosling, I. Haddeland, N. Khabarov, F. Ludwig, Y. Masaki, S. Olin, C. Rosenzweig, A. C. Ruane, Y. Satoh, E. Schmid, T. Stacke, Q. Tang, D. Wisser, Constraints and potentials of future irrigation water availability on agricultural production under climate change. *Proc. Natl. Acad. Sci. U.S.A.* **111**, 3239–3244 (2014).
47. M. Ruiz-Ramos, R. Ferrise, A. Rodríguez, I. J. Lorite, M. Bindi, T. R. Carter, S. Fronzek, T. Palosuo, N. Pirttioja, P. Baranowski, S. Buis, D. Cammarano, Y. Chen, B. Dumont, F. Ewert, T. Gaiser, P. Hlavinka, H. Hoffmann, J. G. Höhn, F. Jurecka, K. C. Kersebaum, J. Krzyszczak, M. Lana, A. Mechiche-Alami, J. Minet, M. Montesino, C. Nendel, J. R. Porter, F. Ruget, M. A. Semenov, Z. Steinmetz, P. Stratonovitch, I. Supit, F. Tao, M. Trnka, A. de Wit, R. P. Rötter, Adaptation response surfaces for managing wheat under perturbed climate and CO_2 in a Mediterranean environment. *Agr. Syst.* **159**, 260–274 (2018).
48. E. Fereres, M. A. Soriano, Deficit irrigation for reducing agricultural water use. *J. Exp. Bot.* **58**, 147–159 (2006).
49. L. Sears, J. Caparelli, C. Lee, D. Pan, G. Strandberg, L. Vuu, C.-Y. C. Lin Lawell, Jevons' paradox and efficient irrigation technology. *Sustainability* **10**, 1590 (2018).
50. F. Stagnari, A. Galieni, S. Speca, G. Cafiero, M. Pisante, Effects of straw mulch on growth and yield of durum wheat during transition to conservation agriculture in Mediterranean environment. *Field Crops Res.* **167**, 51–63 (2014).
51. W. Qin, C. Hu, O. Oenema, Soil mulching significantly enhances yields and water and nitrogen use efficiencies of maize and wheat: A meta-analysis. *Sci. Rep.* **5**, 16210 (2015).
52. B. Biazin, G. Sterk, M. Temesgen, A. Abdulkedir, L. Stroosnijder, Rainwater harvesting and management in rainfed agricultural systems in sub-Saharan Africa—A review. *Phys. Chem. Earth A/B/C* **47-48**, 139–151 (2012).
53. G. C. Nelson, H. Valin, R. D. Sands, P. Havlík, H. Ahammad, D. Deryng, J. Elliott, S. Fujimori, T. Hasegawa, E. Heyhoe, P. Kyle, M. von Lampe, H. Lotze-Campen, D. Mason D'Croz, H. van Meijl, D. van der Mensbrugghe, C. Müller, A. Popp, R. Robertson, S. Robinson, E. Schmid, C. Schmitz, A. Tabeau, D. Willenbockel, Climate change effects on agriculture: Economic responses to biophysical shocks. *Proc. Natl. Acad. Sci. U.S.A.* **111**, 3274–3279 (2014).
54. A. Y. Hoekstra, M. M. Mekonnen, A. K. Chapagain, R. E. Mathews, B. D. Richter, Global monthly water scarcity: Blue water footprints versus blue water availability. *PLOS ONE* **7**, e32688 (2012).
55. R. G. Taylor, B. Scanlon, P. Döll, M. Rodell, R. van Beek, Y. Wada, L. Longuevergne, M. Leblanc, J. S. Famiglietti, M. Edmunds, L. Konikow, T. R. Green, J. Chen, M. Taniguchi, M. F. P. Bierkens, A. MacDonald, Y. Fan, R. M. Maxwell, Y. Yechieli, J. J. Gurdak, D. M. Allen, M. Shamsudduha, K. Hiscock, P. J. F. Yeh, I. Holman, H. Treidel, Ground water and climate change. *Nat. Clim. Change* **3**, 322–329 (2013).
56. D. K. Ray, N. D. Mueller, P. C. West, J. A. Foley, Yield trends are insufficient to double global crop production by 2050. *PLOS ONE* **8**, e66428 (2013).
57. N. D. Mueller, J. S. Gerber, M. Johnston, D. K. Ray, N. Ramankutty, J. A. Foley, Closing yield gaps through nutrient and water management. *Nature* **490**, 254–257 (2012).
58. S. M. Vicente-Serrano, S. Beguería, J. I. López-Moreno, A multiscalar drought index sensitive to global warming: The standardized precipitation evapotranspiration index. *J. Climate* **23**, 1696–1718 (2010).
59. D. P. van Vuuren, J. Edmonds, M. Kainuma, K. Riahi, A. Thomson, K. Hibbard, G. C. Hurtt, T. Kram, V. Krey, J.-F. Lamarque, T. Masui, M. Meinshausen, N. Nakicenovic, S. J. Smith, S. K. Rose, The representative concentration pathways: An overview. *Clim. Change* **109**, 5–31 (2011).
60. N. Ramankutty, A. T. Evan, C. Monfreda, J. A. Foley, Farming the planet: 1. Geographic distribution of global agricultural lands in the year 2000. *Global Biogeochem. Cycles* **22**, GB1003 (2008).
61. W. J. Sacks, D. Deryng, J. A. Foley, N. Ramankutty, Crop planting dates: An analysis of global patterns. *Glob. Ecol. Biogeogr.* **19**, 607–620 (2010).
62. S. Feng, Q. Hu, W. Huang, C.-H. Ho, R. Li, Z. Tang, Projected climate regime shift under future global warming from multi-model, multi-scenario CMIP5 simulations. *Global Planet. Change* **112**, 41–52 (2014).
63. Y. Fan, H. van den Dool, A global monthly land surface air temperature analysis for 1948–present. *J. Geophys. Res.* **113**, D01103 (2008).
64. M. New, M. Hulme, P. D. Jones, Representing twentieth-century space–time climate variability. Part I: development of a 1961–90 mean monthly terrestrial climatology. *J. Climate* **12**, 829–856 (1999).
65. R. G. Allen, L. S. Pereira, D. Raes, M. Smith, *Crop Evapotranspiration-Guidelines for Computing Crop Water Requirements* (FAO Irrigation and Drainage Paper 56, FAO, Rome, 1998).
66. J. Scheff, D. M. W. Frierson, Scaling potential evapotranspiration with greenhouse warming. *J. Climate* **27**, 1539–1558 (2014).
67. M. Collins, R. Knutti, J. Arblaster, J.-L. Dufresne, T. Fichefet, P. Friedlingstein, X. Gao, W. J. Gutowski, T. Johns, G. Krinner, M. Shongwe, C. Tebaldi, A. J. Weaver, M. Wehner, Long-term climate change: Projections, commitments and irreversibility, in *Climate Change 2013: The Physical Science Basis. Contribution of Working Group I to the Fifth Assessment Report of the Intergovernmental Panel on Climate Change*, T.F. Stocker, D. Qin, G.-K. Plattner, M. Tignor, S. K. Allen, J. Boschung, A. Nauels, Y. Xia, V. Bex, P. M. Midgley, Eds. (Cambridge Univ. Press, 2013), pp. 1029–1136.
68. S. Sherwood, Q. Fu, A drier future. *Science* **343**, 737–739 (2014).
69. Q. Fu, S. Feng, Responses of terrestrial aridity to global warming. *J. Geophys. Res. Atmos.* **119**, 7863–7875 (2014).
70. G. van der Schrier, D. Efthymiadis, K. R. Briffa, P. D. Jones, European Alpine moisture variability for 1800–2003. *Int. J. Climatol.* **27**, 415–427 (2007).
71. V. Blauhut, L. Gudmundsson, K. Stahl, Towards pan-European drought risk maps: Quantifying the link between drought indices and reported drought impacts. *Environ. Res. Lett.* **10**, 014008 (2015).

Acknowledgments: We would like to acknowledge the World Climate Research Program Working Group on Coupled Modelling responsible for CMIP5, the climate modeling groups for making the model output available, and P. Štěpánek (CzechGlobe) for valuable comments. We are grateful to the two anonymous reviewers for insightful comments, which improved the structure and clarity of the paper. **Funding:** M.T., J.B., K.K., D.S., J.M., P.H., J.E.O., K.C.K., and U.B. acknowledge support from the SustES - Adaptation strategies for sustainable ecosystem services and food security under adverse environmental conditions (CZ.02.1.01/0.0/0.0/16_019/0000797), which enabled the study to be conducted. S.F. and W.H. were supported by the National Key R&D Program of China (grant no. 2018YFA0606404). International collaboration was also made possible via a framework provided by the international research project FACCE MACSUR. J.E.O. received support from the Innovation Fund Denmark. R.P.R. received support from the SPACES program (grant no. 01LL1304A) of the German Federal Ministry of Education and Research (BMBF). Rothamsted Research received grant-aided support from the Biotechnology and Biological Sciences Research Council Designing Future Wheat Programme [BB/P016855/1]. M.R.-R. was supported by the Spanish National Institute for Agricultural and Food Research and Technology and the Ministry of Economy and Competitiveness (MACSUR02-APCIN2016-00050-00-00). K.C.K. was supported by the German Federal Ministry of Education and Research through MACSUR2 (031B0039C). **Author contributions:** M.T. and S.F. designed the study. M.T., S.F., J.B., D.S., and W.H. performed the experiments. All coauthors analyzed the data and wrote the manuscript. **Competing interests:** The authors declare that they have no competing interests. **Data and materials availability:** All data needed to evaluate the conclusions in the paper are present in the paper and/or the Supplementary Materials. The original water scarcity datasets used in the study are available at https://alpha.czechglobe.cz/mirek. Additional data related to this paper may be requested from the authors as instructed at https://alpha.czechglobe.cz/mirek.

Submitted 21 May 2018
Accepted 3 September 2019
Published 25 September 2019
10.1126/sciadv.aau2406

Citation: M. Trnka, S. Feng, M. A. Semenov, J. E. Olesen, K. C. Kersebaum, R. P. Rötter, D. Semerádová, K. Klem, W. Huang, M. Ruiz-Ramos, P. Hlavinka, J. Meitner, J. Balek, P. Havlík, U. Büntgen, Mitigation efforts will not fully alleviate the increase in water scarcity occurrence probability in wheat-producing areas. *Sci. Adv.* **5**, eaau2406 (2019).